



Magnetic resonance imaging of water vapor absorption in simulated corrugated board

Teemu V. Tuomainen · Jukka Silvennoinen ·
Terhi Mattila · Mikko I. Kettunen ·
Mikko J. Nissi

Received: 22 February 2023 / Accepted: 30 August 2023 / Published online: 13 September 2023
© The Author(s) 2023

Abstract Water vapor absorption into a multi-layer simulated corrugated board structure was investigated using magnetic resonance imaging (MRI). Humidity and other ambient conditions considerably affect the strength and durability of corrugated board, and through creep, collapse of the corrugated board structures at unexpectedly low load levels. Currently, water vapor permeation and absorption are investigated with methods that do not elucidate the behavior of individual sheet layers in corrugated board. With MRI, signal intensity changes caused by water absorption can be spatially located and identified, providing a promising tool for the assessment of internal changes in a board, and its interaction with humidity. In this work, simulated corrugated board assemblies, consisting of alternating straight layers of linerboard and fluting material, were constructed, subjected to one-sided high humidity environment

and periodically MR imaged to obtain temporal information on water accumulation at high relative humidity. It was observed that, in general, the fluting layers would exhibit higher signal intensities sooner, and by extension, higher water accumulation, when compared to the linerboards. The presented study provides insight into the behavior of paperboards in a double-wall corrugated board structure while under constant high humidity. In the future, actual corrugated board samples could be investigated in periodically fluctuating relative humidity and under constant stress to obtain information on the mechanosorptive creep.

Keywords Fluting · MRI · Corrugated board · Water vapor permeation

Introduction

Corrugated board is one of the primary packaging materials for the delivery, storage and international transport of various goods ranging from industrial products to daily consumables and food. In 2020, from the over 25 megatonnes of corrugated material produced in Europe, 43% was used for packaging various food products (European Federation of Corrugated Board Manufacturers (FEFCO) 2020). The overall popularity of corrugated board arises from its many preferable characteristics such as low cost, low weight, high stiffness/strength (with respect to the weight of the material) as well as easy handling

T. V. Tuomainen · M. J. Nissi (✉)
Department of Technical Physics, University of Eastern
Finland, Yliopistonranta 8, POB 1627, 70211 Kuopio,
Finland
e-mail: mikko.nissi@uef.fi

J. Silvennoinen · T. Mattila
Mondi Powerflute Oy, Selluntie 142, 70420 Kuopio,
Finland

M. I. Kettunen
A.I. Virtanen Institute for Molecular Sciences, Kuopio
Biomedical Imaging Unit, University of Eastern Finland,
Neulaniementie 2, 70150 Kuopio, Finland

properties. These characteristics are also evident in the design of corrugated boards. Typical board consists of a three or five layered construction (i.e. single-wall and double-wall corrugated board, respectively), where a corrugated medium is sandwiched between linerboard layers although other constructions exist such as triple and even multi-wall constructions (Berglund et al. 2012). Furthermore, easy and intuitive remanufacturing schemes and good monetary value of the recycled fiber encourage recycling, thus making it environmentally sustainable. Linerboards and corrugated media production from recycled fibers produce less CO₂ than virgin materials (Dominic et al. 2015). Moreover, as with any wood-based material, paper does not cause permanent waste if left unattended in the environment.

Despite the many advantages, the mechanical properties and structural performance of corrugated board degrades with respect to changes in ambient relative humidity (RH) and temperature (Berglund et al. 2012). Thus, strength degradation must be considered in the packaging design. Because of this, corrugated paperboard boxes are typically constructed to be at least 3–8 times stronger (safety factor) (Pathare and Opara 2014) than would be needed if the material were inert to changes in ambient conditions. In other words, the safety factor is used to compensate for the unknown aspects in the environmental lifetime conditions of the corrugated board (Holmvall 2022). Furthermore, a phenomenon known as mechanosorptive creep prevents the paper industry from achieving the best possible theoretical efficiency in packaging; minimal packaging may damage the transported goods while overpackaging increases material and transport costs (Erlöv et al. 2000; Dominic et al. 2015). Therefore, in addition to the scientific benefit, there is a significant industrial and economical need to thoroughly understand the behavior of corrugated board and its constructional elements in variable ambient conditions. If better predictions on the load carrying capability of corrugated board can be made, more optimal packaging designs could be produced. Sustainable packaging is becoming a necessity for both domestic and commercial use, especially through globalization and the growing popularity of e-commerce, so improvements on packaging design can be considered increasingly crucial.

In box manufacturing, corrugated board strength is traditionally evaluated with fast peak strength tests,

namely box compression test, BCT (International Organization for Standardization 1994) or edge crush test, ECT (International Organization for Standardization 2013) that provide a quick estimation of the maximum strength. However, because of the creep phenomenon, knowledge on the long-term load carrying capability of a box and its lifespan under a load is increasingly important. The creep increases in variable ambient humidity conditions and can cause a sudden collapse of a package at an unexpectedly low load level. In cyclic humidity, the actual load level of a corrugated box is found to be less than 30% of the paperboard or corrugated board peak strength (Considine et al. 1989). The importance of creep and the problem it causes has been studied and discussed in many previous publications (Byrd 1972; Leake and Wojcik 1993; Bronkhorst and Riedermann 1994; Dominic et al. 2015; Pathare et al. 2016) with pioneering investigations dating back as far as 1935 (Coffin 2005).

Beyond the mechanical properties of paper, because of the ambient influence, another important and intertwined characteristic is water vapor permeation and absorption. Moisture permeation can be evaluated over a barrier comprising of the paperboard material with different humidity on either side (International Organization for Standardization 2021). In such an experiment, a moisture source (with a known effect on RH) is placed on one side of the sample material, and on the other side the change in %RH is monitored over time using a hygrometer. Thus, the sample material acts as a sealed barrier between the moisture source and the hygrometer. For the investigation of water vapor absorption into a paper sheet, oven drying and gravimetric analysis can be utilized (International Organization for Standardization 2017). However, these methods may be difficult to implement for the temporal investigation of water accumulation in each individual sheet in a multi-layer structure such as corrugated board.

When the ambient conditions change, moisture and temperature gradient is generated through the thickness of the corrugated box wall. Such transient moisture profiles generate heterogenous mechanical properties (Bandyopadhyay et al. 2002). Moisture gradients will cause nonuniform expansion/shrinkage, which in turn will introduce internal stresses to the structures. However, despite extensive research, the knowledge on the effect of moisture gradients on

the moisture accelerated creep is not entirely consistent (Sorvari et al. 2018). To comprehend the moisture variation within paper-based materials, and by extension the creep behavior, various tests and theoretical models (Alfthan and Gudmundson 2005; Strömbro and Gudmundson 2008; Sorvari et al. 2018) have been proposed. Currently, the issue has often been approached by constructing theoretical models considering various aspects of the material properties of paper (inter-fiber and intra-fiber moisture absorption/desorption) and by simulating and monitoring the flux of moisture through a corrugated board and predicting the behavior of the various paper layers. Furthermore, often for simplicity the corrugated board has been treated as one homogenous lump of material, although more accurate models have been developed, such as those presented by Sorvari et al. (Sorvari et al. 2018).

The modelling of multi-layer structures has provided reasonable results in the prediction of creep and moisture distribution in through-thickness direction of corrugated board. Still, the verification of models requires measurements and direct evidence. Information about moisture transport through the board based on mathematical models or gravimetric analysis of the whole board sample does not provide verified information on internal moisture distribution (Leisen et al. 2002). Furthermore, the material composition also affects creep as well as moisture accumulation, and corrugated board can be produced from different compositions and with varying contents of virgin and recycled fibers. As such, the moisture absorption in materials, and as a consequence their individual stiffness and creep resistance, may differ. Knowledge of the actual internal moisture distribution and through-plane diffusion rate could provide valuable information about the composition of corrugated paperboard and optimal packaging design. Thus, novel methods capable of detecting and localizing water distribution inside corrugated board structures are needed to estimate the actual moisture accumulation on, and permeation through paperboards. One method capable of detecting the spatial distribution of water in many different sample types is magnetic resonance imaging (MRI).

MRI is a well-established imaging modality known for its non-invasiveness as well as exquisite and variable soft tissue contrast, numerous pulse sequences and plethora of different image weightings.

These make MRI applicable for the detection of various anatomical structures as well as tissue pathologies and diseases. However, because of its capabilities in detecting, for example free and bound water in materials, its use is not only limited to studies of living things. In this work, we present the MRI of water accumulation in a simulated corrugated board structure and elucidate the usefulness of such investigations. MRI is the spatially encoded extension of a phenomenon known as nuclear magnetic resonance (NMR). In NMR and MRI, a sample is placed in an external magnetic field, excited with radiofrequency pulses and the response of sample nuclei (typically ^1H , *i.e.* a proton) are measured. The signal intensity in a given pixel in a ^1H MR image depends on the proton distribution and density as well as on the electron environment of nuclei together with the used MR imaging parameters (namely repetition time TR and echo time TE). As such, MRI can provide various image-weightings and information on water and proton distribution in an imaged sample. Previous magnetic resonance investigations include drying experiments of pulp (Heikkinen et al. 2006) and cardboards (Harding et al. 2001) as well as moisture accumulation in paper (Leisen et al. 2001, 2002; Bordenave et al. 2007). However, investigations on moisture accumulation in corrugated board are missing.

Materials and methods

In this work, the differences in water vapor uptake of different paperboard materials in a layered structure were investigated with MRI. The measurement setup was designed similarly to previous paperboard moisture permeation studies with MRI (Leisen et al. 2001, 2002) consisting of a source for moisture (liquid water), air cavity and the paper sample although in this work the measurement setup contained a stack of paperboard sheets with a fixed distance between each layer. This multi-layer assembly was constructed to simulate the structure of a double-wall corrugated board.

Simulated corrugated board assembly

The paperboards investigated in this work were 200 g/m² flutings (designated as Fluting A, B, C-a), a 160 g/m² fluting (Fluting C-b) and a 160 g/m²

liner manufactured by a major European paperboard producer (Table 1). Circular disks with a diameter of approximately 5 mm were constructed from the paperboard samples using a hole punch. The samples were stacked inside a PVC (polyvinylchloride) tube together with 3-D printed cylindrical rings as spacers between the paperboard disks to ensure a fixed distance between the paperboards and to avoid direct convection of water (Fig. 1.). Altogether two fluting and three liner paperboard sheets were placed in this configuration (*i.e.* double-wall structure).

For pre-treatment, the paperboard sample stack housed inside a PVC tube was placed into a container with a relative humidity (%RH) of approximately 35% or 75% obtained with a saturated MgCl_2 or NaCl solution, respectively. The temperature and %RH were monitored using an Arduino-based system and a digital relative humidity and temperature sensor (Telaire T9602-3-D, Amphenol Advanced Sensors, St. Mary's, PA) for approximately two weeks prior to MR imaging to ensure adequate time for the humidity in the paperboards to equilibrate (Table 2). All pre-treated paperboard assemblies consisted of an alternating liner-fluting structure consisting of three liners and two flutings. Furthermore, preliminary, non-pretreated paperboard assemblies consisting only of Fluting C-a or C-b (200 or 160 g/m^2 , respectively) as a five-layer structure were investigated with MRI.

After the preparatory steps, the PVC tube containing the paper assembly was sealed on the opposite end using Parafilm M film (Bemis Company,

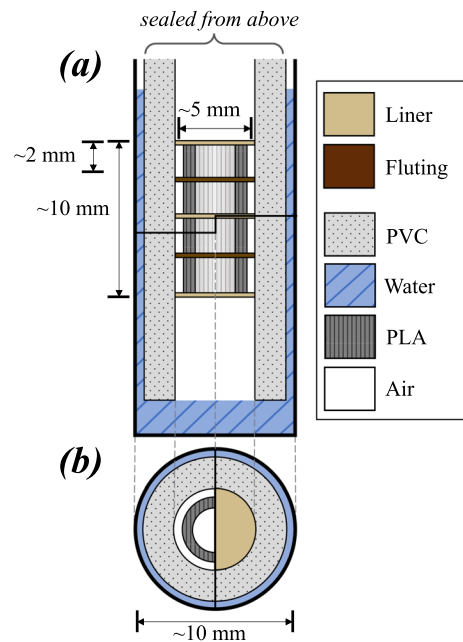


Fig. 1 The experimental setup. Vertical (a) and horizontal (b) cross-section schematics of the measurement setup inside a cylindrical outside diameter 10 mm NMR tube. The paperboard disks (liner and fluting) were vertically stacked inside one end of a PVC tube (polyvinylchloride) and separated with 3-D printed hollow cylinder PLA spacers (polylactic acid) approximately 2 mm in height. The PVC tube was sealed from the other end to avoid water vapor permeation. The paperboard disks and PLA spacers housed inside a PVC tube were placed inside an NMR sample tube with water on the bottom. To avoid water evaporation from the NMR tube, the NMR tube was also separately sealed from the open end

Table 1 Naming convention and information for each paperboard utilized in this work

Designation	Fiber composition	Material properties	Grammage (g/m^2)
Fluting A	Mix fiber fluting, mostly virgin fiber	Sized	200
Fluting B	Mix fiber fluting, mostly virgin fiber	Non-sized	200
Fluting C-a	Virgin fiber semichemical fluting	Non-sized	200
Fluting C-b	Virgin fiber semichemical fluting	Non-sized	160
Liner	Layered mix of virgin and recycled fiber	Sized	160

Table 2 Investigated simulated double-wall corrugated board configurations and their pretreatment conditions (temperature *T* and relative humidity *RH*) presented as average \pm standard deviation (minimum, maximum). All assemblies consisted of

Fluting	T (°C)	RH (%)	Pre-treatment time (days)
Fluting A	21.33 \pm 0.50 (20.81, 23.63)	77.90 \pm 1.76 (75.57, 91.46)	15
Fluting B	21.54 \pm 0.65 (20.96, 24.27)	79.51 \pm 2.35 (74.45, 91.00)	17
Fluting C-a	20.18 \pm 0.75 (19.10, 23.00)	77.77 \pm 1.72 (74.40, 86.38)	14
Fluting C-a	20.47 \pm 0.76 (19.34, 23.10)	35.45 \pm 0.85 (33.94, 39.42)	16

Liner as well as Fluting A, B or C-a. For further information on the composition of the paperboards, the reader is referred to Table 1

Inc., Neenah, WI) and placed inside an outside diameter (O.D.) 10 mm NMR sample tube with deionized water at the bottom (Fig. 1.). The NMR tube was also sealed with Parafilm to minimize water evaporation during MR imaging. Immediately after, the NMR tube containing the paperboard assembly was placed in the MRI scanner after which the device was calibrated.

Magnetic resonance imaging of simulated corrugated board

The MRI was conducted using an 11.7 T vertical magnet with microimaging capabilities (500 MHz Ultrashield, Bruker Biospin GmbH, Rheinstetten, Germany) controlled with the accompanied software (ParaVision 6.0.1. and TopSpin 3.1.). MR imaging was conducted at room temperature using a commercial volume/saddle 10 mm ^1H RF coil housed inside a Micro5 probe (Bruker) with a maximum gradient strength of 3 T/m in all three spatial directions. The MRI scanner was iteratively shimmed and on-resonance frequency (0 Hz) was set to that of the largest and narrowest peak (water). Power was automatically adjusted by the device as water signal was present in the field-of-view (FOV) between the PVC tube and the NMR tube housing. A smaller peak, possibly from PVC tube and/or paperboards, was also observable. Equal receiver gain was set to all consecutive MRI experiments to allow comparison between the time points. The pulse sequence utilized for MRI was a spin echo sequence (rapid acquisition with relaxation enhancement, RARE, with echo train length of one)

with a repetition time (TR) of 1000 ms, and echo time (TE) of 2.1 ms. A single slice with 32 averages was obtained with a slice thickness of 5 mm, and a field-of-view (FOV) of 2 cm \times 1 cm with an isotropic in-plane spatial resolution of 156 μm . The signal evolution in the paperboards was investigated for approximately 40 h between 0.5 and 2-h intervals.

Data analysis

MRI data were processed with MATLAB (R2021b, The MathWorks, Inc., Natick, MA) and with aedes, an in-house built GUI (<http://aedes.uef.fi/>). In the MR images, two reference regions-of-interest (ROIs) were created for background noise and water signal observable between the NMR sample tube and the PVC tube. For each MR image (examples in Fig. 2.), vertical signal profiles were taken as an average of 16 horizontal pixels at the image center. MATLAB findpeaks was utilized for peak detection in the signal profile and in order to extract the signal intensities in the paperboards observed as signal peaks.

Results

Prior to MRI, the layered paperboard assemblies were pre-treated in 35% or 75% relative humidity (RH) using saturated MgCl_2 and NaCl solutions, respectively. For 75% RH pre-treated paperboard, water vapor uptake can be clearly observed at the beginning of the experiment, as well as a clear increase in the paperboard as a function of time (Fig. 2). Furthermore, when compared to linerboards, higher signal

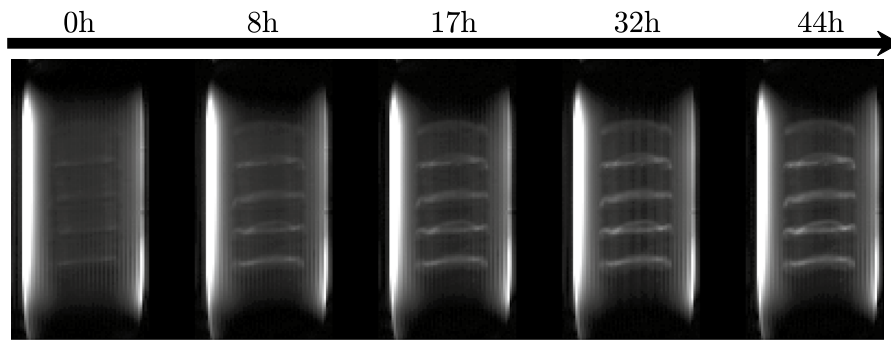


Fig. 2 Temporal signal evolution in paperboards with MRI. MR images of the simulated corrugated board assembly with Fluting B at different timepoints in water vapor conditions. For further information on the simulated corrugated board assem-

bly the reader is referred to Fig. 1 and Table 1. Bright signal areas on the left and right sides of the MR images are from liquid water between the NMR tube and PVC tube

intensities in the fluting material are visible (Fig. 3), suggesting that more water is present in fluting. Similar signal behavior is observable with 35% RH pre-treatment using saturated MgCl_2 .

To illustrate the signal development and thus water accumulation in the paperboards, the signal intensities at the peaks from the signal profiles (Fig. 3) were investigated as a function of time (Fig. 4). As can be observed from Fig. 4, after high %RH pre-treatment, the first fluting layer seems to accumulate more moisture (higher signal intensity in MRI) than the first linerboard sheet even though the liner is closer to the liquid waterfront. Similar observation can be made for low %RH pre-treatment (Fig. 4d.)

Investigation of non-pretreated multi-layer stack assemblies consisting of varying grammage fluting are presented in Fig. 5. For the higher grammage assembly (with Fluting C-a, 200 g/m^2), the signal intensity behaves more linearly, as more signal is observable near the liquid water and less further away from it. However, such linear interaction is not observable with the lower grammage Fluting C-b (160 g/m^2).

Discussion

Noticeable signal increase was observed with respect to time for each individual sheet inside a simulated corrugated board (Fig. 2). It was observed that the signal generated in the fluting materials was generally higher than for the liners, suggesting that the fluting material may absorb more water than surrounding

linerboards (Figs. 3 and 4). As wet or moist papers have reduced load-carrying capabilities, during moisture permeation fluting materials may lose more strength than is generally expected, and thus, their quality and composition should be carefully considered. For the linerboard furthest from the water source, minimal signal increase is observable. This may be to an extent caused by the limited range of the RF coil with some contribution from a smaller moisture gradient experienced by the third linerboard compared to other linerboards.

The signal generated from the paperboards is clearly visible as a function of time. Moreover, signs of saturation of the signal intensity over a duration of 40 h is observable (Fig. 4). The presented data may be used to simulate water permeation and absorption in each individual sheet, which in turn could provide insight into the moisture profiles and creep properties of paperboards in corrugated board structures. Furthermore, the addition of alternating ambient conditions could provide valuable insight into the absorption, desorption, and permeation of water in each individual sheet structure in corrugated board. The assembly consisting of the fluting C-a and linerboard sheets was investigated with two separate pre-treatment conditions, 75%RH and 35%RH using saturated NaCl and MgCl_2 solutions, respectively. Although the preconditions were different prior to MRI, the MR images exhibit similar signal evolution (Fig. 3c and d) with higher signal from the first fluting sheet than the first liner sheet. Moreover, it should be noted that the time scales between the two experiments are different, with MgCl_2 pretreated assembly experiment

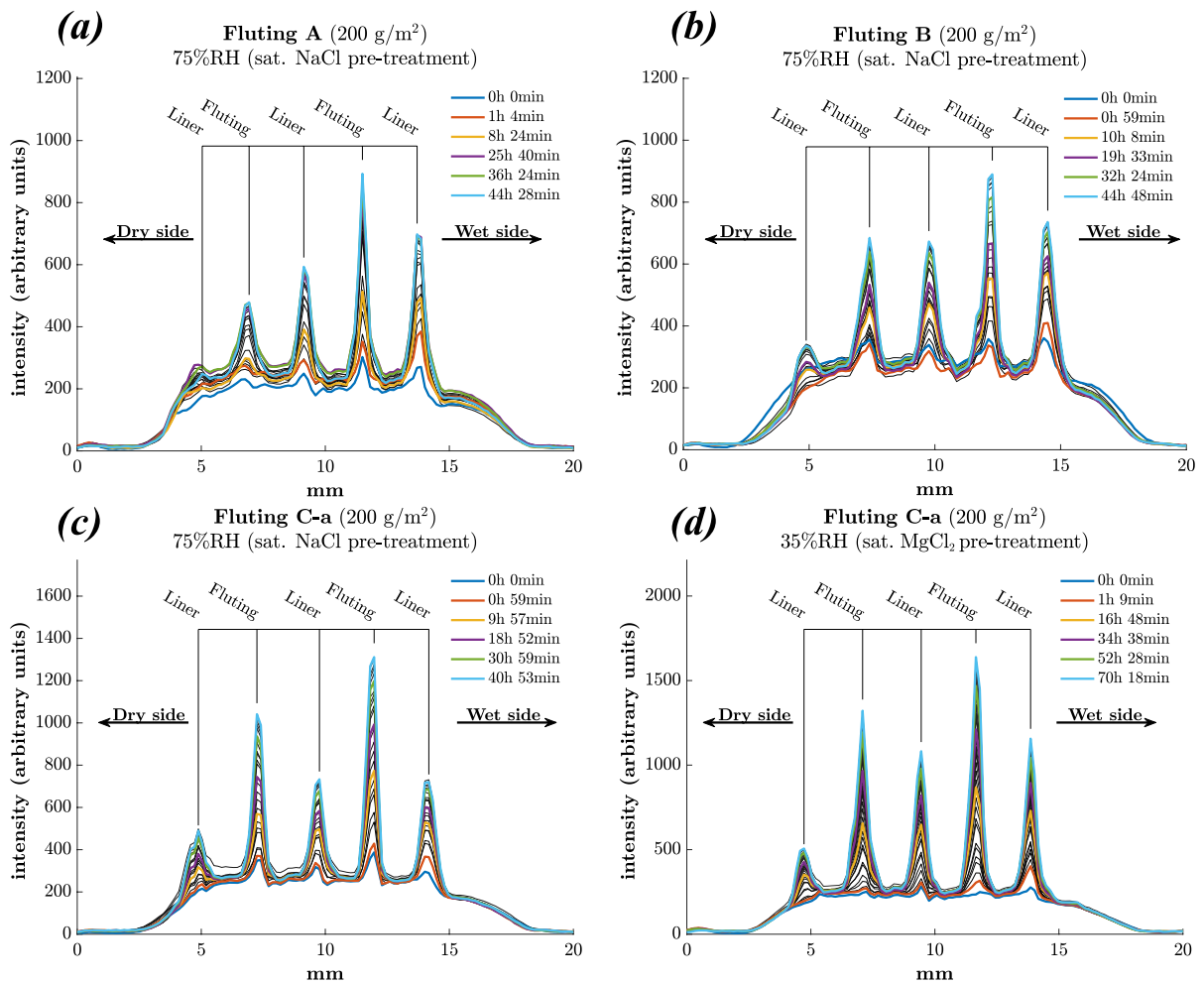


Fig. 3 MRI signal intensity profiles of different simulated corrugated board assemblies. Evolution of the signal intensity profile of simulated corrugated board with assemblies with Fluting A (a), Fluting B (b) and Fluting C-a (c–d). All the measurements are presented using black lines, with the six

highlighted timepoints presented using different colors and a larger linewidth. Please note the differing time points for the highlighted measurements. For the composition of the corrugated board assemblies, reader is referred to Table 1. For the actual pre-treatment data, reader is referred to Table 2

lasting longer. With all profiles, some form of signal peaks are observable at the beginning of the experiment (Fig. 3) with clear increase as a function of time, as illustrated in (Fig. 4).

For assemblies with Fluting A and B, the second fluting layer (Fluting 2, in Fig. 4a and b) does not surpass the second linerboard (Liner 2) at any time point. For the assembly with Fluting B, however, the signal evolution of the second fluting layer approaches the second linerboard (Fig. 4b). For Fluting C-a, however, irrespective of the pre-treatment, this phenomenon is observable; the second fluting layer signal

surpasses that of the second linerboard. As material differences are present between the fluting materials (Table 1), the behavior may be caused by such differences. For example, the Fluting A material is sized (*i.e.* more hydrophobic) whereas Fluting B or C-a are not. This in turn may cause the differences in the observable signal increase in Fluting 2. Furthermore, Fluting C-a consists of virgin fiber compared to the mixed composition of Fluting A and B, and as such some properties of the flutings may have been altered, including water permeation.

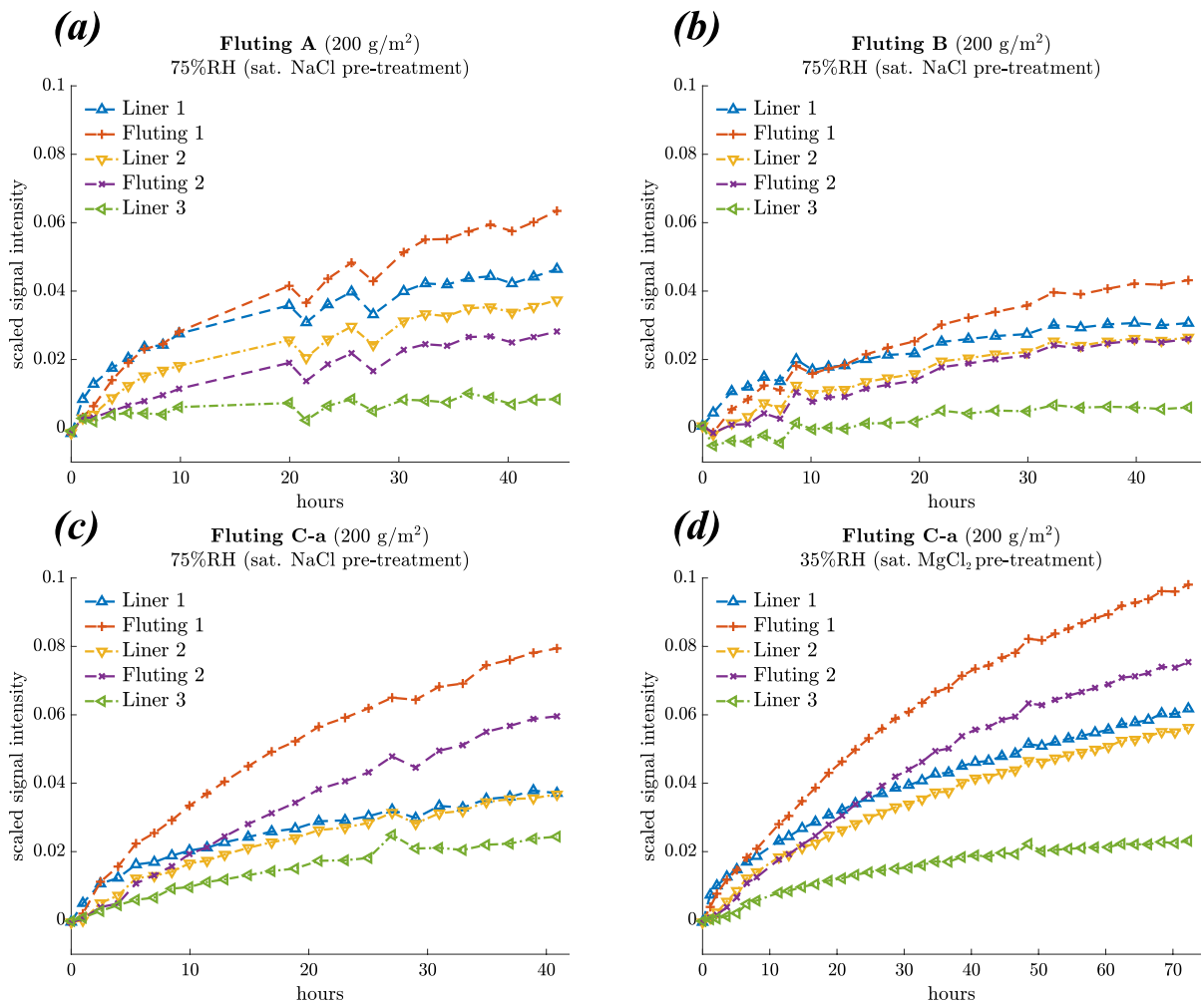


Fig. 4 Signal evolution of paperboards with respect to time. Signal intensity evolution at the location of the observed peaks (paperboard layers) using simulated corrugated board assemblies with Fluting A (a), Fluting B (b) and Fluting C-a (c–d). Signal intensities have been scaled to background noise (mini-

mum) and signal from water (maximum) for each time point using min–max normalization. For the composition of the assemblies, reader is referred to Table 1. For the actual pre-treatment data, reader is referred to Table 2

When compared to the other paperboards, the last linerboard (Liner 3 in Fig. 4) exhibits minimal signal evolution. This is intuitively understandable as this paperboard is furthest from the water vapor source. As such the water vapor gradient over the last linerboard is not as high as for other paperboards in the assembly. It should be noted, however, that this paperboard is also closer to the edge of the range of the RF coil. As such the observed signal behavior may be a result of a combination of these two phenomena.

Although clear signal generation is observable, some limitations are present in the proposed

simulated structure and study design. First, the corrugated media could not be implemented due to the narrow bore size (diameter of 10 mm with the used RF coil) of the MRI scanner and consequently an even smaller paperboard sample diameter. Actual 5 mm diameter corrugated board samples could not be used as the wavelength of the corrugated media would have been longer than the sample diameter. As such, corrugated board was not used due to practical reasons and to allow focus on the vapor permeation and absorption without potentially confounding geometric factors. Because of this, an approximation of

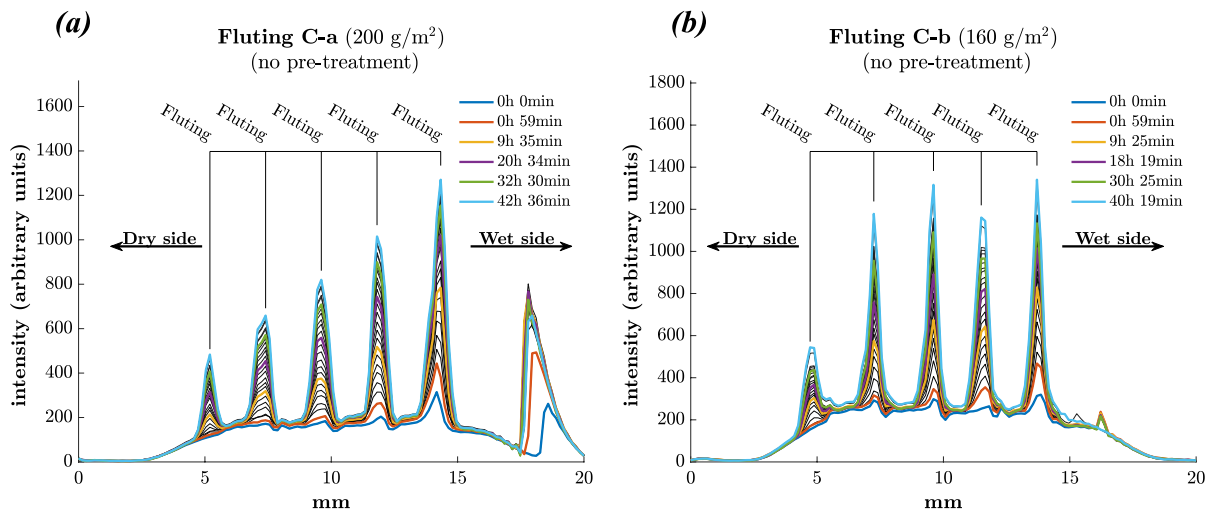


Fig. 5 Signal intensity profiles of non-pretreated simulated corrugated board assemblies. Profiles of non-pretreated board assemblies consisting only of Fluting C-a (a) and Fluting C-b

(b) with grammage 200 or 160 g/m², respectively. Liquid water signal is observable in subfigure (a) at approximately 17–20 mm

a corrugated medium was used by implementing a fixed 2 mm distance between the paperboards using cylindrical spacer rings. While this design avoids direct contact between fluting and liner paperboards, the design was not entirely contactless between the paperboards (via the 3-D printed spacers). In the actual corrugated board structure, the liner and corrugated medium are attached to one another with adhesive which could also prevent, or at least limit, direct moisture convection. Another limitation is the relative humidity obtained with distilled water. Because no salts were used in the MRI experiments, the relative humidity is theoretically 100%. Furthermore, because of only a small amount of liquid at the bottom of the NMR tube, it may be depleted during the long experiment due to its accumulation to the paperboards and elsewhere. Finally, all materials were kept in identical environments during the experiment, but the previous ambient humidity history experienced by the investigated paperboards was not excessively controlled.

Some of the imaged sample assemblies were pre-treated in a controlled relative humidity (%RH) using saturated salt solutions for approximately two weeks. However, variation in the numeric values of %RH was observable. The observed variation is most likely caused by the measurement sensor, as the %RH may be calibrated, by the sensor, using the temperature value, i.e. the sensor may use the temperature

to correct the measured %RH, which in turn induces some lag and changes in the relative humidity value reported by the sensor upon changes in the ambient temperature.

The presented method provides noticeable signal increase with respect to time, but as stated in the introduction, the measured ¹H MRI signal is a superposition of the proton density (i.e. water content) and NMR relaxation phenomena, the proportions of which are dependent on the imaging parameters. Thus, the obtained signal intensity may not be linear with water content or concentration, and a more complex description may be needed. Since the signal in ¹H MRI is generated from any material with hydrogen nuclei, for example, the hydroxyl (OH) groups in the cellulose may generate observable signal. Furthermore, as the electron environment of ¹H causes a contribution to the detectable signal, the expansion of the cellulose matrix may increase signal generated by the OH groups amplifying the changes detected. It should also be noted that the absolute signal values, even when scaled to the water reference, are not entirely comparable between the measurements, but the temporal evolution of the signal curves within a single experiment are comparable. Nevertheless, the most likely cause for the observable signal increase is the absorption and accumulation of water vapor into

the paperboards. In Fig. 5, fluting-only assemblies were investigated with no humidity pre-treatment. It can be observed that the signal profiles with a larger grammage (Fluting C-a, 200 g/m²) behave more linearly than those with a smaller grammage (Fluting C-b, 160 g/m²). As such the thickness of the paperboards may affect the observed signal intensities in the investigated paperboard assemblies.

Previous studies related to the assessment of paperboard, cardboard and pulp interactions with water using magnetic resonance techniques have, to our understanding, primarily revolved around MRI during drying (Harding et al. 2001; Leisen et al. 2001; Heikkinen et al. 2006) and on rarer cases, on MRI during moisture absorption using a humidity source and a high grammage (two sheets of 468 g/m² pressed to form 936 g/m²) sheet of paper (Leisen et al. 2002). Moreover, assessment of water absorption on paper sheets with relaxation time measurements using NMR spectroscopy have been performed (Bordenave et al. 2007), i.e. without spatial information. In contrast, the current study presents a novel measurement technique and spatially resolved magnetic resonance imaging scheme on water vapor absorption on a multi-layer assembly of paperboards. In this work, MRI was used to assess the accumulation of moisture into liner and fluting layers of a simulated corrugated board. Current evaluation methods for water absorption include the “static gas” method where humidity increase caused by moisture on one side is measured on the opposite side of the investigated structure (International Organization for Standardization 2021). Other methods include oven-drying and gravimetric methods where the weight difference is utilized to estimate water accumulation (International Organization for Standardization 2017). Whereas these investigative methods rely on total water accumulation or permeation, MRI provides novel insight into the internal structures and behavior of multi-layer paperboard assemblies. Thus, MRI could be utilized in scientific studies and industrial research and development, as it can provide spatial information on the water accumulation and internal water content. However, its use in daily, continuous monitoring of moisture can be rather impractical. In the future, larger bore size MRI scanner and actual corrugated board material could be used together with a more controlled humidity environment to obtain

more realistic information on the water permeation. It should be noted however, that larger bore size in practice leads to smaller field strengths, poorer SNR and limited image resolution in the allotted time which could hinder the possibilities for such approach.

Conclusions

Magnetic resonance imaging can be used to detect moisture accumulation on various layers of a simulated corrugated board structure. Although other mechanisms, such as NMR relaxation, may at least to an extent affect the signal formation, the proton density can be correlated with water accumulation. Further investigations with MRI are needed to obtain information on humidity on liner and fluting materials with respect to mechanosorptive creep. In the future, the presented data could be used to simulate and model water absorption in a multi-layer paperboard structure, and corrugated board could be investigated with MRI in alternating ambient conditions.

Acknowledgments This work was carried out with the support of Kuopio Biomedical Imaging Unit, University of Eastern Finland, Kuopio, Finland (part of Biocenter Kuopio, Finnish Biomedical Imaging Node, and EuroBioImaging). The authors gratefully acknowledge the support from Dr. Tuomo Savolainen for the help in the relative humidity and temperature measurements.

Author contributions Conceptualization: TVT, JS, TM, MIK, MJN; Methodology: TVT, JS, TM, MIK, MJN; Formal analysis and investigation: TVT, MJN; Writing—original draft preparation: TVT, JS, MJN; Writing—review and editing: TVT, JS, TM, MIK, MJN; Funding acquisition: TVT, MIK, MJN; Resources: TVT, JS, TM, MIK, MJN; Supervision: MIK, MJN.

Funding The research was financially supported by the Niemi Foundation, Finnish Cultural Foundation, Jenny and Antti Wihuri Foundation, Academy of Finland (Grant Nos. 285909 and 325146) and European Regional Development Fund and Pohjois-Savo Regional Council (grants A73998 and A74016). Open access funding provided by University of Eastern Finland (UEF) including Kuopio University Hospital.

Data availability Data are made openly and fully available at the Zenodo repository (<https://doi.org/10.5281/zenodo.6952566>).

Declarations

Competing interests The authors declare no competing interests.

Open Access This article is licensed under a Creative Commons Attribution 4.0 International License, which permits use, sharing, adaptation, distribution and reproduction in any medium or format, as long as you give appropriate credit to the original author(s) and the source, provide a link to the Creative Commons licence, and indicate if changes were made. The images or other third party material in this article are included in the article's Creative Commons licence, unless indicated otherwise in a credit line to the material. If material is not included in the article's Creative Commons licence and your intended use is not permitted by statutory regulation or exceeds the permitted use, you will need to obtain permission directly from the copyright holder. To view a copy of this licence, visit <http://creativecommons.org/licenses/by/4.0/>.

References

- Alfthan J, Gudmundson P (2005) Linear constitutive model for mechano-sorptive creep in paper. *Int J Solids Struct* 42:6261–6276. <https://doi.org/10.1016/j.ijsolstr.2005.06.029>
- Bandyopadhyay A, Ramarao BV, Ramaswamy S (2002) Transient moisture diffusion through paperboard materials. *Coll Surf A Physicochem Eng Asp* 206:455–467. [https://doi.org/10.1016/S0927-7757\(02\)00067-5](https://doi.org/10.1016/S0927-7757(02)00067-5)
- Berglund L, Carlsson L, Coffin DW et al (2012) Mechanics of paper products. De Gruyter, Boston
- Bordenave N, Grelier S, Pichavant F, Coma V (2007) Water and moisture susceptibility of chitosan and paper-based materials: structure-property relationships. *J Agric Food Chem* 55:9479–9488. <https://doi.org/10.1021/jf070595i>
- Bronkhorst CA, Riedermann JR (1994) The creep deformation behaviour of corrugated containers in a cyclic moisture environment. In: Fellers C, Laufenberg TL (eds) Proceedings of the moisture induced creep behaviour of paper and board. Stockholm, p 249–273
- Byrd VL (1972) Effect of relative humidity changes on compressive creep response on paper. *Tappi J* 55:1612–1613
- Coffin DW (2005) Review: the creep response of paper. In: Advances in paper science and technology, Trans. of the XIIIth Fundamental Research Symposium. Cambridge, p 651–747
- Considine JM, Thelin P, Gunderson DE, Fellers C (1989) Compressive creep behavior of paperboard in a cyclic humidity environment— exploratory experiment. *Tappi J* 72:131–136
- Dominic CAS, Östlund S, Buffington J, Masoud MM (2015) Towards a conceptual sustainable packaging development model: a corrugated box case study. *Packag Technol Sci* 28:397–413. <https://doi.org/10.1002/pts>
- Erlöv L, Sörås A, Lövgren C (2000) Packaging and the prevention of environmental impact. Packforsk, Denmark
- European Federation of Corrugated Board Manufacturers (FEFCO) (2020) FEFCO Annual Statistics 2020
- Harding SG, Wessman D, Stenström S, Kenne L (2001) Water transport during the drying of cardboard studied by NMR imaging and diffusion techniques. *Chem Eng Sci* 56:5269–5281. [https://doi.org/10.1016/S0009-2509\(01\)00197-X](https://doi.org/10.1016/S0009-2509(01)00197-X)
- Heikkinen S, Alvila L, Pakkanen TT et al (2006) NMR imaging and differential scanning calorimetry study on drying of pine, birch, and reed pulps and their mixtures. *J Appl Polym Sci* 100:937–945. <https://doi.org/10.1002/app.23051>
- Holmvall M (2022) Predicting creep lifetime performance in edgewise compression of containerboards and for stacked corrugated board boxes. *Packag Technol Sci* 35:53–67. <https://doi.org/10.1002/pts.2607>
- International Organization for Standardization (1994) ISO 12048:1994 Packaging—Complete, filled transport packages—Compression and stacking tests using a compression tester
- International Organization for Standardization (2013) ISO 3037:2013 Corrugated fibreboard — Determination of edgewise crush resistance (unwaxed edge method)
- International Organization for Standardization (2021) ISO 9932:2021 Paper and board—determination of water vapour transmission rate of sheet materials—dynamic sweep and static gas methods. Switzerland
- International Organization for Standardization (2017) ISO 287:2017 Paper and board—determination of moisture content of a lot—Oven-drying method
- Leake C, Wojcik R (1993) Humidity cycling rates: how they influence on container lifespan. *Tappi J* 76:26–30
- Leisen J, Hojjatie B, Coffin DW et al (2002) Through-plane diffusion of moisture in paper detected by magnetic resonance imaging. *Ind Eng Chem Res* 41:6555–6565. <https://doi.org/10.1021/ie0204686>
- Leisen J, Hojjatie B, Coffin DW, Beckham HW (2001) In-plane moisture transport in paper detected by magnetic resonance imaging. *Dry Technol* 19:199–206. <https://doi.org/10.1081/DRT-100001361>
- Pathare PB, Berry TM, Opara UL (2016) Changes in moisture content and compression strength during storage of ventilated corrugated packaging used for handling apples. *Packag Res*. <https://doi.org/10.1515/pacres-2016-0001>
- Pathare PB, Opara UL (2014) Structural design of corrugated boxes for horticultural produce: a review. *Biosyst Eng* 125:128–140. <https://doi.org/10.1016/j.biosystemseng.2014.06.021>
- Sorvari J, Leppänen T, Silvennoinen J (2018) The effect of the through-thickness moisture content gradient on the moisture accelerated creep of paperboard: hygro-viscoelastic modeling approach. *Nord Pulp Pap Res J* 33:122–132. <https://doi.org/10.1515/npprj-2018-3001>
- Strömbro J, Gudmundson P (2008) An anisotropic fibre-network model for mechano-sorptive creep in paper. *Int J Solids Struct* 45:5765–5787. <https://doi.org/10.1016/j.ijsolstr.2008.06.010>

Publisher's Note Springer Nature remains neutral with regard to jurisdictional claims in published maps and institutional affiliations.